System Architecture of a CubeSat re-entry Mission

Quinn R.W. Kupec* and Natalie M. Condzal†, Jessica W. Bleich ‡, and Adrian N. Danao-Schroeder§
University of Maryland, College Park, MD, 20742

Since CubeSats were invented in the late 1990s, they have revolutionized the aerospace industry. Their small size has allowed for quicker development of short-term space research, but could also be used as a method of sample return if designed to allow for re-entry into Earth's atmosphere. To date, no CubeSat has ever re-entered Earth's atmosphere in a controlled manner as it would burn up in the atmosphere due to its small size and insufficient shielding. However, we propose a mission profile that combines the use of an ultra-low ballistic coefficient entry decelerator and heat shield that would result in a successful CubeSat re-entry and recovery. A 3U CubeSat with this system would have an expected ballistic coefficient of approximately 23 kg/m^2, compared to the normal ballistic coefficient of a 3U CubeSat of 70 kg/m^2. With this drastically decreased ballistic coefficient, we would expect a 3U CubeSat to be able to successfully re-enter Earth's atmosphere. We propose ejecting a re-entry vehicle in the form factor of a 3U CubeSat and a 12U service module that is launched from the International Space Station. This paper presents results from aerothermodynamic and re-entry profile analyses associated with our proposed flight path; a datasheet survey to asses feasible materials; and a test plan to ensure the flight-readiness of the CubeSat.

I. Nomenclature

3U	=	3 unit CubeSat standard dimensions (10 cm × 10 cm × 30 cm)
12U	=	12 unit CubeSat standard dimensions (23 cm × 24 cm × 36 cm)
α	=	Angle of Attack
β	=	Ballistic Coefficient
I_{sp}	=	Specific impulse
L/D	=	Lift to drag ratio
P_0	=	Stagnation pressure
T_0	=	Stagnation temperature

II. Introduction

While systems have been developed and used to deorbit a CubeSat, none have been used to allow the CubeSat to be recovered intact. These systems have primarily focused on reducing orbital debris through the re-entry of CubeSats. As such, there was no need for it to survive re-entry. It was therefore preferable that the vehicle did not survive so as to reduce risk to those on the ground. Instead, we propose a concept that can both deorbit a CubeSat, as well as allow for a survivable re-entry of the vehicle where it could then be recovered.

The ISS currently has a down-mass capability limited to two vehicles: Soyuz and Cargo Dragon. While Crew Dragon, Starliner, and eventually Dream Chaser will provide more down-mass capability in the future, the ISS will still be limited to the schedules of these vehicles. A re-entry capable CubeSat could be deployed from the ISS at anytime and would allow for small down-mass capability relatively unconstrained by the schedule of visiting vehicles. This CubeSat

*Undergraduate researcher, University of Maryland Department of Aerospace Engineering, 3179 Glenn L. Martin Hall Bldg No. 088, 4298 Campus Drive, University of Maryland,College Park, MD 20742, AIAA Student Member

†Undergraduate researcher, University of Maryland Department of Aerospace Engineering, 3179 Glenn L. Martin Hall Bldg No. 088, 4298 Campus Drive, University of Maryland,College Park, MD 20742, AIAA Student Member

‡Undergraduate researcher, University of Maryland Department of Aerospace Engineering, 3179 Glenn L. Martin Hall Bldg No. 088, 4298 Campus Drive, University of Maryland,College Park, MD 20742, AIAA Student Member

§Undergraduate researcher, University of Maryland Department of Aerospace Engineering, 3179 Glenn L. Martin Hall Bldg No. 088, 4298 Campus Drive, University of Maryland,College Park, MD 20742, AIAA Student Member

could be deployed from already existing systems on the ISS, such as the NanoRacks CubeSat Deployer (NRCSD), which uses the Kibo Module's Airlock.

This same capability could be harnessed for free flying CubeSat missions as well. It would allow for scientific missions requiring a sample return to take place without having to go to the ISS. The CubeSats could be deployed as part of a ride share launch and then deorbit and re-enter once the scientific mission is complete. Concepts have also been proposed for a CubeSat sized vehicle which could be used for interplanetary exploration [1]. These concepts use a re-entry system similar to the one proposed here to enable atmospheric entry on other planets as well as sample return to Earth.

III. Concept of Operations

The proposed system would consist of a 12U CubeSat service module and a re-entry vehicle based on the 3U CubeSat form factor. The re-entry vehicle will be housed inside the service module for the on-orbit portion of the mission. The re-entry vehicle will sit inside of the service module until after the deorbit burn is completed, at which point the re-entry vehicle will deploy its heat shield to prepare for a safe re-entry into Earth's atmosphere.

While missions have been considered with a deployment from a ride-share mission, this paper will primarily focus on the ISS mission case. For initial demonstration missions, the re-entry vehicle would already be attached to the service module when launched. For operational missions to the ISS, the astronauts would place the items to be returned to the Earth into the re-entry vehicle. They would then insert the re-entry vehicle into the service module before it is ejected from the ISS. On the ISS, the NRCSD releases CubeSats through the airlock in the Kibo Module [2]. The NRCSD can support CubeSats up to the 12U form factor and launches them into a 51.6° inclination orbit at approximately 400 km altitude. Normally, CubeSats are loaded into the NRCSD before being launched to the ISS. Special considerations would need to be made for this mission or they would have to be deployed using another system. The NanoRacks Bishop Airlock, slated to launch to the ISS in late 2019 or early 2020, would provide additional capability for CubeSat deployment from the ISS [3]. This system will allow individual CubeSats and smallsats to be placed in the airlock by the crew on the ISS before being ejected.

Once at a safe distance from the ISS, the vehicle will power on and begin system checks. The payload will down link data over the Iridium satellite network. If the system checks show that the vehicle is functioning nominally, it will begin the deorbit procedure. From there, the re-entry vehicle will separate from the service module and begin its re-entry into Earth's atmosphere. The deorbit maneuvers will be conducted to target a specific landing location. A specific landing location has not been selected yet with the two main options under consideration being an ocean landing preferably close to the US coast, or a landing in the Utah Test and Training Range (UTTR). Other CubeSat re-entry systems have also proposed a landing in the UTTR, in part because it simplifies the recovery of the CubeSat [4]. It also simplifies any security issues with the recovery of the payload since it would land in the US. A water landing would necessitate the addition of a flotation system on the vehicle. Either location would require the use of a parachute once the vehicle is subsonic for final descent and landing. Currently, we are working towards a landing of the payload in the UTTR, but a final decision has not been reached.

IV. Deorbiting System

We are currently exploring two options for CubeSat deorbiting systems, a propulsive deorbit and aerobraking. For a propulsive deorbit, the vehicle only needs to conduct one burn to lower its perigee to a point where drag from the heat shield will allow it to rapidly deorbit. As such there is little need for a complex throttle-able propulsion system. This allows for a small solid rocket motor to be used. There are a variety of options for commercially-available solid rocket motors that can be used on CubeSat missions. A downside of solid rocket motors is their inherent thrust misalignment [5]. Since the vehicle would need to be equipped with an attitude control system (ACS) for deployment of the re-entry vehicle, the thrust misalignment could be corrected. Currently we are basing our design and analysis off of the Northrop Grumman STAR 4g motor. The STAR 4g provides just enough thrust to deorbit the vehicle and has a very small form factor. By using a solid rocket motor, the payload could be re-entered shortly after being released from the ISS, thus minimizing return time of samples for an operational mission. The solid rocket motor does pose a problem for the ISS mission case, as special considerations would need to be made for its handling. Likely, the CubeSat could not be brought inside the station due to the hazardous nature of the motor. However, its simplicity and effectiveness still make it worth considering.

The second option for deorbiting the vehicle is an aerobraking system. Proposals for similar CubeSat re-entry

missions have proposed using the heat shield for aerobraking [6]. However, this significantly complicates the heat shield design as it requires that the heat shield can be opened to varying degrees. This eliminates the use of a spring loaded mechanism as it only has one deployment state. As such an alternate aerobraking system would be used. The Drag De-Orbit Device (D3) developed by University of Florida Advanced Autonomous Multiple Spacecraft Lab uses 4 3.7m long tape-spring booms to create drag for the payload [7]. The booms significantly decrease the ballistic coefficient allowing the spacecraft to lower its orbit. However, the D3 device is designed for a 3U CubeSat and would be significantly less effective on the 12U service module/re-entry vehicle combo. The Exo-Brake was designed to deorbit CubeSats specifically for ISS sample return [4, 8]. The system is able to provide deorbit capability for larger CubeSats as well as a targeted landing zone. The Exo-Brake system can provide enough accuracy to land the re-entry vehicle within the UTTR as well as a landing zone off either coast of the US [4, 8]. The Exo-Brake's design is significantly more complex than the solid rocket motor as it requires special systems for its deployment and control [4]. In the interest of designing the simplest system for CubeSat re-entry, this paper will focus on the solid rocket motor deorbiting system.

V. System Concepts

The design of the system is divided into two components, the re-entry vehicle and the service module. This allows for the re-entry module to remain small as it does not need to contain all the systems for on-orbit operations. It also allows for easy interface with a CubeSat dispenser without interference with the heat shield. So far the majority of development efforts have been focused on the heat shield design as it is the most mission critical piece of the design. The heat shield is fixed in place to the forward end of the re-entry vehicle and encapsulates the vehicle when the shield is collapsed.

A. re-entry Vehicle

The re-entry vehicle is based off of a 3U CubeSat mounted behind the heat shield. This CubeSat would contain all systems necessary for re-entry and landing, such as actuators for the heat shield, communications systems, and parachutes/flotation devices depending on the targeted landing location. The re-entry module will also contain a compartment for sample return. Once the vehicle is separated from the service module, it will use an independent ACS to ensure it is oriented correctly for re-entry. Figure 1 depicts a CAD model of this concept with the heat shield deployed. The heat shield deploys using spring loaded hinges attached to each of the eight spars. Once the re-entry vehicle separates from the service module, the shield will be released from its stowed configuration, Fig. 2, and a locking mechanism will engage. In its stowed configuration, the vehicle is slightly larger than the 3U form factor with a stowed diameter of 14 cm and length of 33 cm. Since the re-entry vehicle is deploying from the 12U service module, a strict adherence to the 3U CubeSat form factor is not necessary. This allowed for more flexibility in the design and the maximization of volume for the payload that trails the heat shield.

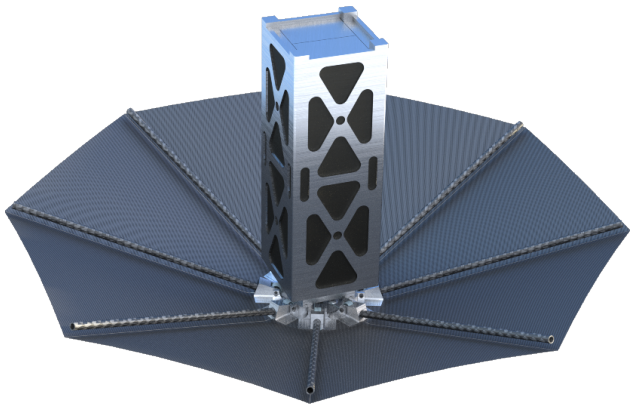

Fig. 1 re-entry vehicle concept based on a 3U CubeSat

A number of commercial options are available for a 3U CubeSat structure. However, given the need to interface with the heat shield and to house a parachute, and possibly a flotation system, the structure of the re-entry vehicle's payload would likely be custom manufactured. The aft portion of the structure would house a system to interface with the service

Fig. 2 re-entry vehicle concept based on a 3U CubeSat with heat shield stowed

module. This system would handle the physical connection between the modules, as well as data and power transmission. Concepts were considered that did not have an electrical connection, but rather used a short range mesh network for communication between the service module and re-entry vehicle. However, these concepts were eliminated as a result of the need for power transmission between the service module's solar panels and the re-entry vehicle's battery.

B. Heat Shield

The design of the heat shield for the re-entry module is based on previously developed concepts for ultra-low ballistic coefficient (ULβ) entry vehicles. Specifically, our chosen configuration of a mechanically actuated heat shield is derived from the ParaShield concept [9, 10]. While the ParaShield was designed using a spherical configuration, the designs are fairly similar none the less. Our chosen blended sphere cone shape provides a larger projected area, thereby lowering the ballistic coefficient. It also allows for a more compact folded volume. Previous concepts for CubeSat re-entry vehicles have proposed a similar heat shield design. However, they considered a heat shield with a 60° half angle sphere-cone inflatable heat shield [11]. While an inflatable shield simplifies the structural design of the heat shield, it adds significant complexity to the overall vehicle design. In addition, the heat shield fabric needs to have 0% porosity to maintain pressure within the shield. This puts more constraints on the fabric options for the shield. It also adds the possibility of the heat shield deflating during re-entry causing a catastrophic failure of the system. The chosen 70° half angle blended sphere-cone shape builds off of legacy designs with this same configuration such as the Mars Viking Lander [12].

While there have been concerns about the stability of this shape in subsonic regimes of flight, our previous testing with the TARDIS* system has shown that this is not the case. Figure 3 shows the results of the drop test of the TARDIS-2 system which also used a 70° half angle blended-sphere cone heat shield shape. Our results showed that the vehicle remained within +/- 5° of the heat shield down orientation. We plan to drop test the exact configuration that would be uses on the CubeSat mission, and expect similar results to the TARDIS-2 flight test.

The heat shield attached the eight spars to fabric gores and a spherical nose cap to provide its shape. A concept of this design is shown in Fig. 4. An exact material for the spars has not been selected, but a carbon fiber composite would be preferable given its stiffness and low thermal conductivity. The nose cap would also be a composite structure covered with a thermal protection system (TPS) to handle the high stagnation point temperatures. The details of the TPS for both the fabric and the nose cap will be discussed further in the Aerothermodynamics section.

*TARDIS stands for Triggered Aerodynamic Resistance and Drag by Increase in Surface

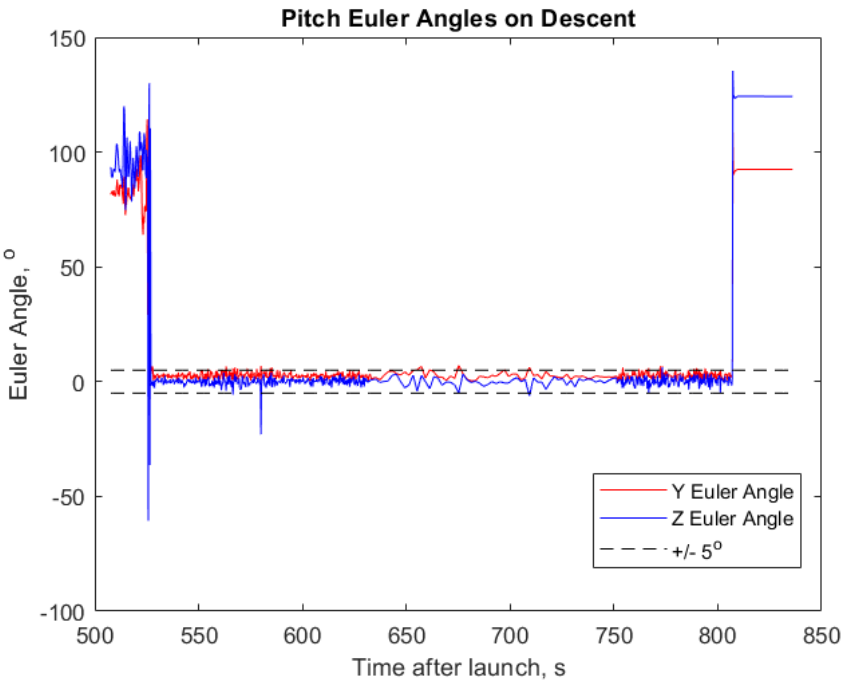

Fig. 3 Pitch angles during drop tests of TARDIS-2 with 70° half angle blended sphere-cone shape

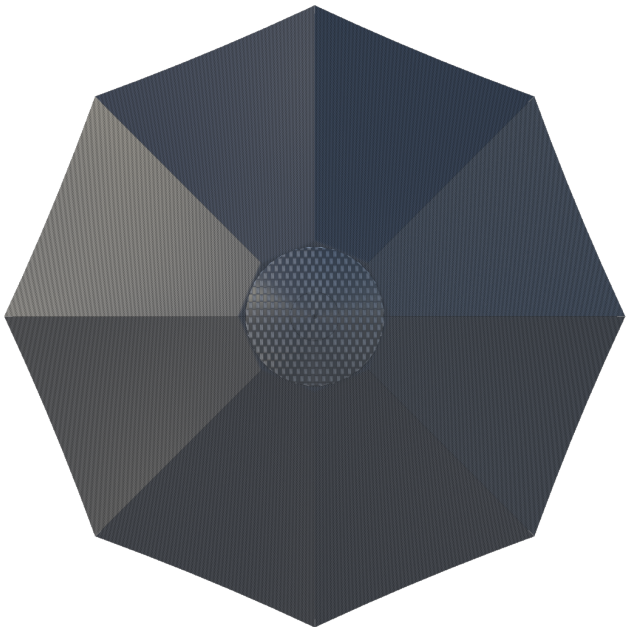

Fig. 4 CAD model of the heat shield concept

C. Service Module

The service module contains all the systems needed for on-orbit operations. Its design adheres to the 12U CubeSat form factor. Given its relatively simple function, the design of the service module will build heavily off previously flown 12U CubeSats, with the majority of the design effort being focused on the interface between the two vehicles. The primary functions of the service module are to interface with the CubeSat dispenser, provide deorbiting capability, attitude control, and to provide power for both modules while in orbit. Figure 5 shows a concept of the service module

that houses the re-entry module prior to deployment. For simplicity's sake, the solar panels would be positioned on four sides to eliminate the need for attitude control for the majority of the flight. With the service module designed to be disposed of upon re-entry, no thermal protection considerations are made for the module.

A commercially available structure also would not be viable for the service module. Since the re-entry vehicle is housed in the center of the service module, too many modifications would need to be made to a commercial structure for it to be more practical than a custom structure. A locking mechanism located towards the aft end of the module would hold the re-entry vehicle in place until the completion of the deorbit burn at which point the electrical connections would be severed and springs would push the re-entry vehicle away from the service module. Since the primary communications system is housed inside of the re-entry module, an auxiliary antenna would need to be mounted to the module. The use of a transparent patch antenna would allow for greater flexibility in the attitude of the vehicle as well as in antenna placement [13].

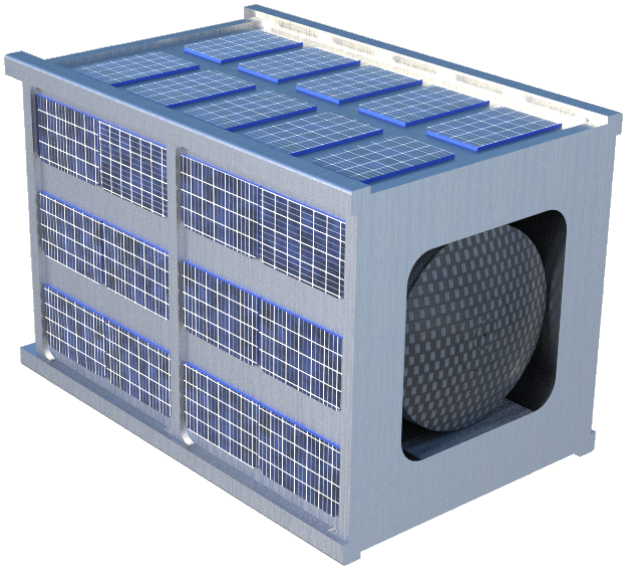

Fig. 5 Service module with the re-entry module housed inside

VI. On-orbit Operations

The power for the combined service module/re-entry vehicle system will be generated by solar panels mounted to the exterior of the service module. Power will be stored in a battery located inside the re-entry vehicle. With the service module being discarded after ejecting the re-entry vehicle, there is no need for a separate battery on the module. With a sufficient number of solar panels mounted on the outside of the service module, both the service module and re-entry vehicle will receive constant electrical power while in orbit. There are multiple commercial off-the-shelf options for CubeSat solar panels that can connect with rechargeable batteries to allow the lifetime of a mission to increase from only a few days to a few months. Additionally, using commercial off-the-shelf solar panels, especially for 12U CubeSats, will help to greatly reduce costs and design effort. The rechargeable battery used on CubeSat missions is typically Li-ion or Li-polymer, as both are commercially available and meet the energy requirements needed for CubeSat missions. Additionally, Lithium batteries have low self-discharge, maintain high-valued cell voltage, and do not have a memory effect when used for extended life cycles. As such, Lithium batteries are the best option for rechargeable batteries to power the re-entry vehicle and service module. [14]

The communications system will consist of an Iridium module that will provide reliable satellite communications. This will allow for the payload to maintain communications with the ground even when it is not flying over a ground station [15]. It will also enable easy communications with the payload throughout re-entry and after landing. The communications system will be mounted in the re-entry vehicle and will make use of the auxiliary antenna mounted to the service module for communications while on-orbit.

Both the re-entry vehicle and the service module will require an ACS. Given the large size and mass of the system, the commonly used magnetic torque rods would not be practical. As such, the system would use a cold gas ACS

for the re-entry vehicle and service module. Isobutane has a good I_{sp} for maneuvering and is considered a "green" propellant and thereby has minimal safety procedures for handling [16]. The ACS on the service module will stabilize the spacecraft after being ejected from the CubeSat dispenser. Once the spacecraft is stabilized, there will be no specific attitude control requirements until the deorbit burn. Before the burn, the ACS will align the motor on the CubeSat to burn in the retrograde direction. Throughout the burn and until the ejection of the re-entry vehicle, the ACS on the service module will keep the CubeSat steady in this orientation. Once the re-entry vehicle is ejected, the ACS on the service module will be disabled and will be allowed to tumble during its re-entry and eventual breakup. The ACS on the re-entry vehicle will keep the spacecraft oriented at α=10° until the transition to an α=0°.

VII. re-entry Profile

The re-entry profile for the vehicle is based off an ISS ejection and a deorbit burn using the STAR 4g solid rocket motor. It is assumed that the deorbit burn would be conducted at the orbit's perigee, possible resulting in extended on-orbit loiter time to wait for the trajectory to line up with the intended landing location. The re-entry profile was modeled using the FreeFlyer orbital dynamics software and the MSIS-2000 atmospheric model. Figure 6 shows the expected entry profile of the vehicle. The re-entry vehicle enters the atmosphere with α=10°. The vehicle then transitions to α=0° at an altitude of 20 km. By entering the atmosphere with a high angle of attack, the vehicle is able to decrease the peak aerodynamic loading. With the re-entry vehicle's β=23kg/m^2 and approximate L/D=.025, it will experience a maximum deceleration of approximately 10 g's[10]. Table 1 shows the coefficients for varying angles of attack of the re-entry vehicle.

The design of the re-entry vehicle's heat shield allows it to be descending sub Mach 1 by 20 km without the use of another decelerator. The vehicle's Mach number once entering the atmosphere[†] is shown in Fig. 7. Since the vehicle is able to slow below Mach 1 on its own, a subsonic parachute can be used for final descent and landing, thereby reducing the complexity of the vehicle's design.

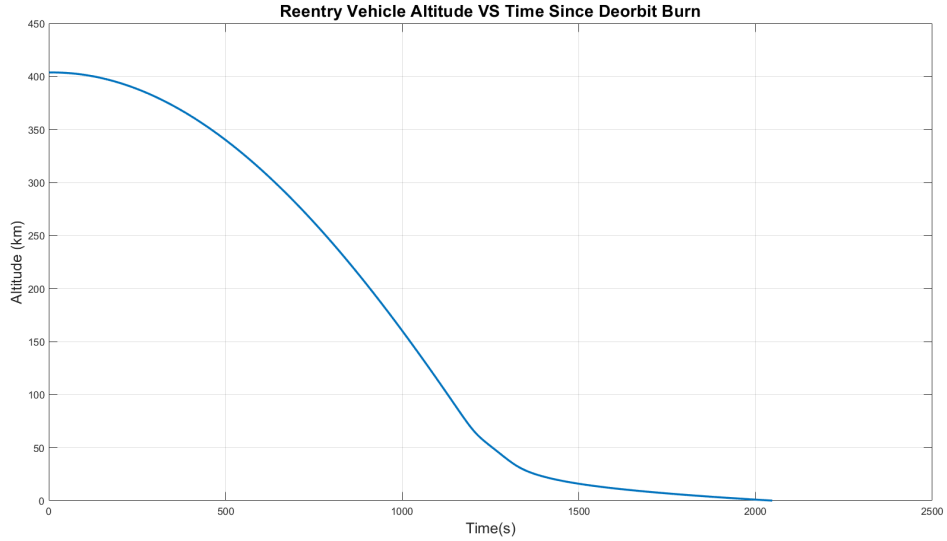

Fig. 6 Altitude profile for the re-entry vehicle

VIII. Aerothermodynamics

Computational Fluid Dynamics (CFD) analysis was performed on the re-entry vehicle using ANSYS Fluent to determine its aerodynamic properties. The model was set up using a kω Shear Stress Transport model for viscosity. Cases were run at varying α between 0° and 10° and between Mach 1.5 and Mach 6. Due to the limited computational capability of our version of ANSYS, analysis was not able to be conducted above Mach 6. Figure 9 and Fig. 10 show some of the results of this analysis. One of the key areas of concern for the re-entry vehicle is wake impingement on the

[†]Entering the earth's atmosphere is being defined as the vehicle crossing the Von Karman line

Table 1 Coefficients for re-entry vehicle at varying α

α	C_l	C_d	L/D
0	0	1.50	0
5	0.035	1.28	0.027
10	0.031	1.29	0.025

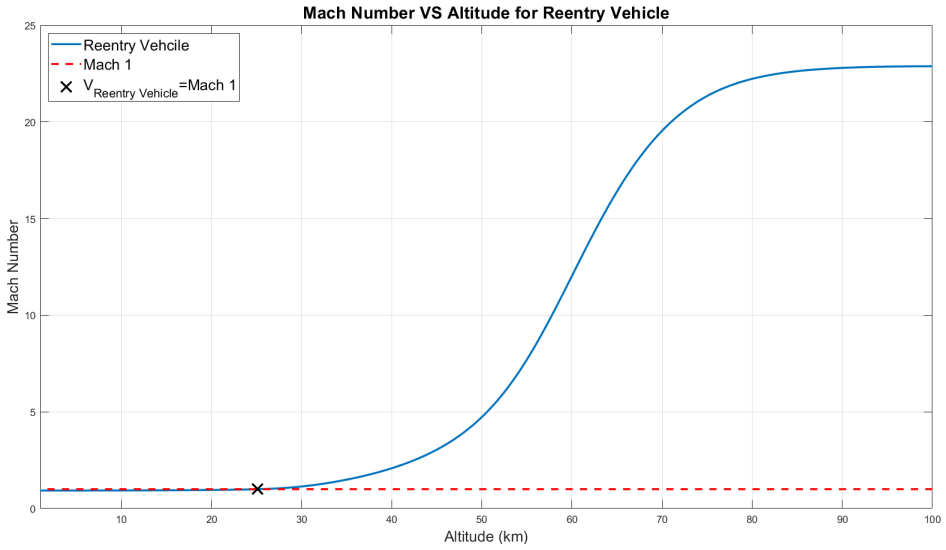

Fig. 7 Vehicle's Mach number following atmospheric entry

payload at high velocity. As shown in Fig. 10 the wake closes significantly aft of the vehicle so wake impingement will not be an issue. The CFD analysis also shows our expected stagnation pressure to be 10.2 kPa at Mach 6. Assuming isentropic flow, we can expect a peak T_0 of approximately 30 000 K and a peak P_0 of 1215 GPa. Figure 8 shows T_0 and P_0 throughout the re-entry vehicle's descent, assuming isentropic flow. Given that the isentropic flow assumption breaks down for very high Mach numbers, the values for peak stagnation temperature, and especially stagnation pressure may not be accurate. However, they provide a good baseline for the design. The stagnation temperature and pressure should be centered on the spherical nose cap, although the α=10° will offset this some.

To account for the high T_0 the heat shield, TPS will be composed of high temperature fabric and a phenolic impregnated carbon ablator (PICA) coating on the spherical nose cap, t he rest of the shield will be composed of a combination of two fabrics, Nextel 312 AF-12 and Beta Cloth. The PICS heat shield phenolic resin and low density carbon fiber provide thermal protection for the surface it is applied to [17]. A PICA heat shield with a density of .266 g/cm^3 has a thermal conductivity of 2.78E-03 W K/cm at a temperature of 3333 K [17]. This indicates that an aerodynamic nose cap coated with PICA would be able to handle the high stagnation temperatures expected.

Key considerations for the TPS fabrics are permeability and temperature resistance. As Magazu et. al. explain, the permeability of the fabric relates to the shock-layer flow seepage in the shield[18]. This seepage can cause adverse heating on the payload, thereby defeating the purpose of the heat shield for thermal protection. The analysis conducted by Magazu et. al. show that a seepage of 1% of the shock-layer volume is the maximum allowable value while maintaining heat shield effectiveness [18]. The Nextel 312 AF-12 fabric has a higher porosity value [19] than acceptable. However, if backed with Beta Cloth, a fabric with acceptable porosity values [20], the shock-layer seepage can be eliminated. The Nextel fabric is still needed in the design as its higher thermal resistance and low conductivity [19] protect the Beta Cloth which has a low melting point [20]. To achieve the desired temperature and shock-layer seepage values, multiple layers of each fabric would be used [18].

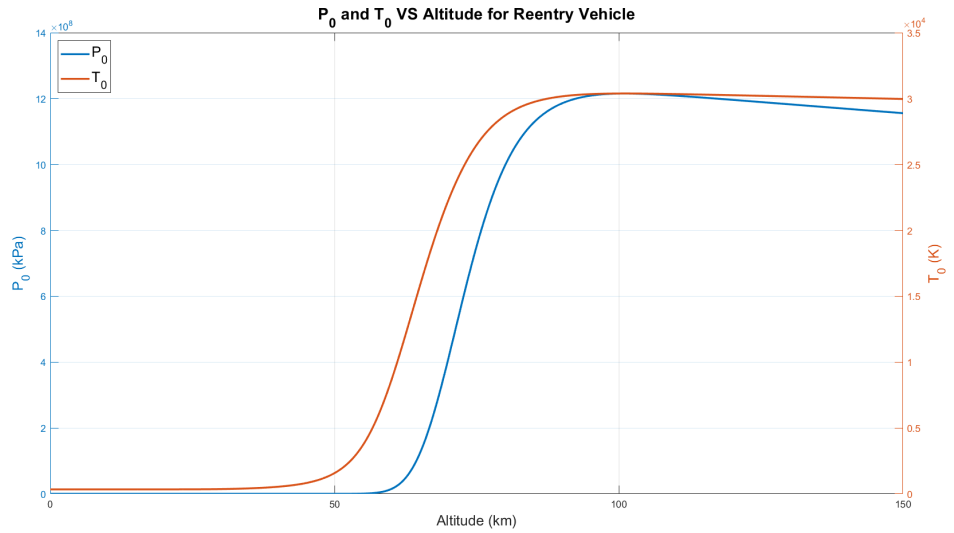

Fig. 8 re-entry vehicle's stagnation temperature and pressure assuming isentropic flow

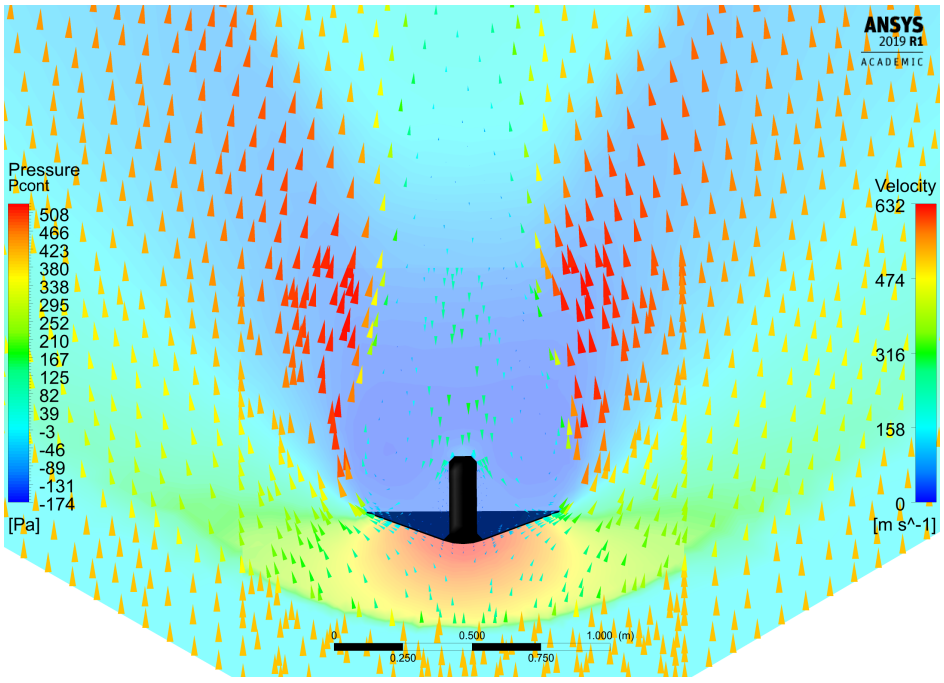

Fig. 9 re-entry vehicle's velocity vectors and pressure at α = 0 in a Mach 1.5 flow

IX. Future Work

In order to test the operation of the re-entry system, we will first construct a mock-up of the re-entry vehicle to be tested using a high altitude balloon drop. These tests are expected to take place within the next year. For the first test launch, the payload will be released from a balloon at 3 km. Provided this test is successful, we plan to test the system again with drops at 15 km and 25 km. This data will help us validate the aerodynamic stability of the payload in its sub Mach 1 flight regime. Another key portion of these tests is the parachute deployment system. The balloon drop test article will use a parachute system similar to what is planned for the re-entry vehicle. The design of the heat shield induces trailing vortices at the aft of the vehicle. The balloon flight tests will allow us to determine if the parachute can be ejected in a way so as to avoid interference from the vortices.

Following the completion of the balloon flight tests we plan to work on the development of the service module.

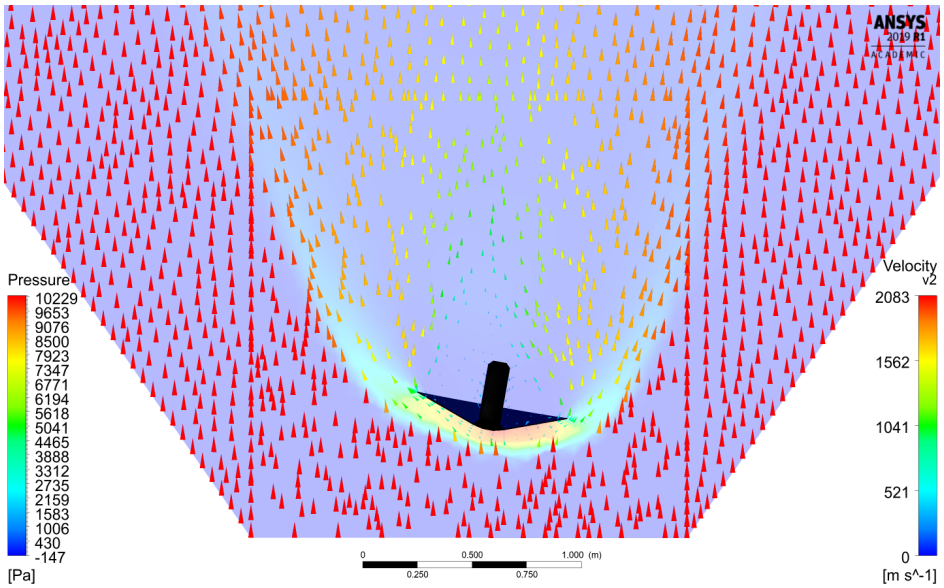

Fig. 10 re-entry vehicle's velocity vectors and pressure at α = 10 in a Mach 6 flow

Its electrical and communication systems will need to be developed and tested along with the re-entry vehicle release system. Further analysis will also need to be conducted to make a final decision on the deorbiting system. Factors relating to the launch of the vehicle may determine which system is selected. Once these decisions are made and a launch is confirmed, construction on the flight versions of the service module and re-entry vehicle will begin.

We also plan to conduct further thermodynamic analyses on the re-entry vehicle. A higher power computational system will be used to conduct CFD analyses on the re-entry vehicle up through Mach 22. A higher fidelity aerodynamic model will also be created that takes high temperature air dissociation into account.

X. Conclusion

While presently no CubeSats have successfully re-entered Earth's atmosphere, such a mission is possible using technology that is currently available. Through the use of a ULβ decelerator, a re-entry vehicle approximately the size of a 3U CubeSat can re-enter the atmosphere and safely land. By consolidating on-orbit functionality to a service module, the mission plan can be significantly simplified and thus time of development shortened. Provided that the systems described here could be developed, a CubeSat re-entry mission would be feasible within a few years.

Acknowledgments

Thank you to the MD Space Grant Consortium for their funding for this research. Thank you to Dr. Mary Bowden and Dr. Dave Akin for their continued support for this project. Thank you to the rest of the TARDIS team for your work in this research.

References

[1] Cassell, A. M., Smith, B., Wercinski, P., Ghassemieh, S., Hibbard, K., Nelessen, A., and Cutts, J., "ADEPT, A Mechanically Deployable Re-Entry Vehicle System, Enabling Interplanetary CubeSat and Small Satellite Missions," *32ndAnnual Small Satellite Conference*, 2018, pp. 1–9.

[2] Woellert, K., "NanoRacks CubeSat Deployer," 2019.

[3] Hodge, M., "NanoRacks Bishop Airlock: Payload Capabilities, Your Commercial Gateway to Space," *ISS Research and Development Conference*, 2018.

[4] Dutta, S., Bowes, A. L., Cianciolo, A. D., Glass, C. E., and Powell, R. W., "Guidance Scheme for Modulation of Drag Devices to Enable Return from Low Earth Orbit," *AIAA SciTech Forum*, 2017, pp. 1–11.

[5] Kevin L. Zondervan, D. R. B. H. C. K. S.-H. C. P. M. T. S., Jerry Fuller, and Kremer, A., "CubeSat Solid Rocket Motor Propulsion Systems providing Delta-Vs greater than 500 m/s," *28th Annual AIAA/USU Conference on Small Satellites*, 2014, pp. 1–2.

[6] Carandente, V., and Savino, R., "New Concepts of Deployable De-Orbit and Re-Entry Systems for CubeSat Miniaturized Satellites," *Recent Patents on Engineering, Vol. 8, No. 1*, 2014, pp. 2–10.

[7] Omar, S., DiMauro, G., Martin, T., and Bevilcqua, "CubeSat Mission to Demonstrate Aerodyanmically Controlled Re-Entry using the Drag De-Orbit Device (D3), Enabling Interplanetary CubeSat and Small Satellite Missions," *32nd Annual Small Satellite Conference*, 2018, pp. 1–17.

[8] Murbach, M. S., Papadopoulos, P., Glass, C., Dwyer-Cianciolo, A., Powell, R. W., Dutta, S., Guarneros-Luna, A., Tanner, F. A., and Dono, A., "Modeling the Exo-Brake and the Development of Strategies for De-Orbit Drag Modulation," *AIAA Space Forum*, 2016.

[9] Akin, D. L., "Applications of Ultra-Low Ballistic Coefficient Entry Vehicles to Existing and Future Space Missions," *SpaceOps Conference*, 2010, pp. 1–12.

[10] Akin, D. L., "The ParaShield Entry Vehicle Concept: Basic Theory and Flight Test Development," *Annual AIAA/Utah State University Conference on Small Satellites*, 1990, pp. 1–11.

[11] Andrews, J., Watry, K., and Brown, K., "Nanosat Deorbit and recovery System to Enable New Missions," *Annual AIAA/Utah State University Conference on Small Satellites*, 2011, pp. 1–5.

[12] Willcockson, W. H., "Mars Pathfinder Heatshield Design and Flight Experience," *Journal of Spacecraft and Rockets*, Vol. 36, No. 3, 1999, pp. 374–379.

[13] Neveu, N., Garcia, M., Casana, J., Dettloff, R., Jackson, D. R., and Chen, J., "Transparent Microstrip Antennas for CubeSat Applications," *IEEE International Conference on Wireless for Space and Extreme Environments*, 2013.

[14] Bugryniec, P., "CubeSat: The Need for More Power to Realise Telecommunications," 2016, p. 3.

[15] Muri, P., and McNair, J., "A Survey of Communication Sub-systems for Intersatellite Linked Systems and CubeSat Missions," *Journal of Communications, Volume 7, No. 4*, 2012, p. 295.

[16] Cardin, J. M., Coste, K., Williamson, D., and Gloyer, P., "A Cold Gas Micro-Propulsion System for CubeSats," *Annual AIAA/Utah State University Conference on Small Satellites*, 2003.

[17] Covington, M. A., Heinemann, J. M., GoldStein, H. E., Chen, Y. K., Terrazas-Salinas, I., Balboni, J. A., Olejniczak, J., and Martinez, E. R., "Performance of a Low Density Ablative Heat Shield Material," *Journal of Spacecraft and Rockets*, Vol. 36, No. 3, 1999, pp. 374–379.

[18] Magazu, H. K., Lewis, M. J., and Akin, D. L., "Aerothermodynamics of a Parashield Re-Entry Vehicle," *Journal of Spacecraft and Rockets*, Vol. 36, No. 3, 1999, pp. 374–379.

[19] Division, M. A. M., "3M™ Nextel™ Ceramic Fabrics 312 and 440," 2018.

[20] Finckenor, M. M., and Dooling, D., "Multilayer Insulation Material Guidelines," *NASA NTRS*, 1999.